Environmental Microbiology
August 2011, Volume 13, Issue 8, pages 2078–2091
http://dx.doi.org/10.1111/j.1462-2920.2011.02425.x

Methanogenic diversity and activity in hypersaline sediments of the centre of the Napoli mud volcano, Eastern Mediterranean Sea

Cassandre Sara Lazar[1], R. John Parkes[2], Barry A. Cragg[2], Stéphane L'Haridon[1], Laurent Toffin[1,*]

[1] Laboratoire de Microbiologie des Environnements Extrêmes, UMR 6197, Ifremer Centre de Brest, Département Etudes des Environnements Profonds, Université de Bretagne Occidentale, BP70, 29280 Plouzané, France
[2] School of Earth and Ocean Sciences, Cardiff University, Main Building, Park Place, Cardiff CF103YE, UK

*: Corresponding author : Laurent Toffin, Tel. (+33) 2 98 22 43 96 ; Fax (+33) 98 22 47 57 ;
email address : laurent.toffin@ifremer.fr

Abstract :

Submarine mud volcanoes are a significant source of methane to the atmosphere. The Napoli mud volcano, situated in the brine-impacted Olimpi Area of the Eastern Mediterranean Sea, emits mainly biogenic methane particularly at the centre of the mud volcano. Temperature gradients support the suggestion that Napoli is a cold mud volcano with moderate fluid flow rates. Biogeochemical and molecular genetic analyses were carried out to assess the methanogenic activity rates, pathways and diversity in the hypersaline sediments of the centre of the Napoli mud volcano. Methylotrophic methanogenesis was the only significant methanogenic pathway in the shallow sediments (0–40 cm) but was also measured throughout the sediment core, confirming that methylotrophic methanogens could be well adapted to hypersaline environments. Hydrogenotrophic methanogenesis was the dominant pathway below 50 cm; however, low rates of acetoclastic methanogenesis were also present, even in sediment layers with the highest salinity, showing that these methanogens can thrive in this extreme environment. PCR-DGGE and methyl coenzyme M reductase gene libraries detected sequences affiliated with anaerobic methanotrophs (mainly ANME-1) as well as *Methanococcoides* methanogens. Results show that the hypersaline conditions in the centre of the Napoli mud volcano influence active biogenic methane fluxes and methanogenic/methylotrophic diversity.

INTRODUCTION

Large amounts of the greenhouse gas methane are stored in marine sediments (Kvenvolden, 1988). Methane is also emitted from these sediments, sometimes ascending from deep sources along channels or conduits reaching the seafloor, creating structures such as pockmarks or mud volcanoes. Submarine mud volcanoes are typically found at various tectonically active and passive continental margins, from which mud and fluids (water, brine, gas, oil) flow or erupt (Milkov, 2000). They are considered a significant source of atmospheric carbon, especially methane (Dimitrov, 2003). Mud volcanoes are typically driven by overpressured subsurface sediment in subduction zones of continental margins. They can erupt violently or gently extrude semi-liquid mud-volcano breccia (Dimitrov, 2003). Over 200 mud volcanoes have been found along the northern flank of the Mediterranean Ridge in the eastern Mediterranean Sea (Charlou et al., 2003). The formation of the Mediterranean Ridge is linked to the collision between the African and Eurasian tectonic plates, resulting in intensive faulting (Haese et al., 2006). The Napoli mud volcano is a circular dome situated in the Olimpi area (Fig. 1). This mud volcano has ascending brine fluids characterized by pools and lakes with diameter size ranging from centimeters to meters (Charlou et al., 2003). Fauna are present on the summit (active inner zone), whereas in the outer zone most fauna are dead, suggesting that chemosynthetic activity is limited due to the brines and fluid flows (Olu-Le Roy et al., 2004).

Most of the gas venting from these mud volcanoes is composed of methane, mainly of biogenic origin (Charlou et al., 2003) which is produced by methanogenic ***Archaea***. Methanogenesis is the ultimate terminal oxidation process in the anaerobic degradation of organic matter. Methanogens are divided into three metabolic groups based on substrates used: hydrogenotrophs use H_2/CO_2, acetoclasts use acetate, and methylotrophs use methylated compounds (Garcia et al., 2000). Few studies have specifically focused on activity or diversity of methanogens in cold seeps and mud volcanoes (Dhillon et al., 2005; Kendall et al., 2006), and only eight methanogens belonging to six different genera have been cultured and isolated from cold seeps (Sowers et al., 1983, 1984, von Klein, 2002, Mikucki et al., 2003, Shlimon et al., 2004, Singh et al., 2005, Kendall et al., 2006, 2007). Most (>90%) of the uprising methane is consumed by anaerobic oxidation of methane (AOM) before it reaches the seafloor (Knittel et al., 2009). AOM is driven by methanotrophic ***Archaea***

(ANME), and is often coupled to ***Desulfosarcinales***- and ***Desulfobulbus***-related bacteria, as sulfate-reducing partners (Boetius et al., 2000; Knittel ***et al.***, 2005; Niemann et al., 2006). Based on the 16S rRNA gene phylogeny, AOM in marine environments is mediated by three distinct clusters of ***Euryarchaeota***, namely ANME-1, ANME-2 and ANME-3. These clusters are phylogenetically related to the orders ***Methanosarcinales*** and ***Methanomicrobiales*** which include cultivated methanogens (Lösekann et al., 2007).

The maximum activity of a mud volcano is generally located at the center where methane-rich muds and fluids are freshly expelled from a deep reservoir. In Napoli, methane to ethane ratios and $\delta^{13}CH_4$ values (-65.6‰PDB, Charlou et al., 2003) indicate that methane is biogenic. Napoli mud volcano deep-sourced brine fluids (Charlou et al., 2003) impact on the geochemistry, and thereby, potentially microbial diversity and activities. However, the methanogenic community diversity and activity in the active centers of mud volcanoes has not yet been described. Hence in this study, pathways for biogenic methane production, community structure and activities of methanogens in the center of the Napoli mud volcano were assessed. Rates of the three main metabolic types of methanogenesis were measured, together with the distribution of ***Archaea***, including methanogens by 16S rRNA gene PCR-DGGE, as by the functional ***mcrA*** gene of methanogens/methanotrophs.

RESULTS and DISCUSSION

Geochemistry of hypersaline sediments in the center of the Napoli mud volcano.

The temperature at shallow depths of both KUL-3 and KUL-4 gravity cores in the centre of Napoli was an average of 14 °C, with a gradient of 100°C/km (Jean-Paul Foucher, pers. comm.). This value was low compared to high gradients of mud volcanoes of the Nile Deep-Sea Fan (***e.g***. sediment temperatures were higher than 40 °C at 10 mbsf at the center of the Isis mud volcano, Feseker et al., 2009), indicating that Napoli is a cold mud volcano with moderate fluid flow rates. Chloride concentrations increased with depth (Fig. 2), from 1578 mM in surface sediments (3 times higher than seawater), to 5085 mM at 122 cmbsf sediment layers (~10 times higher than seawater). Profiles of the Mg^{2+} and Ca^{2+} porewater concentrations (Supplementary Material. SM1) decreased with depth indicating authigenic carbonate precipitation between 0 and 60 cmbsf probably due to anaerobic oxidation of

methane (AOM) increasing alkalinity (Chaduteau, 2008). The Na^+ porewater concentrations profile (Supplementary Material. SM1) increased with depth, and was clearly correlated with the Cl^- profile. Porewater sulfate concentrations initially decreased rapidly with depth, indicating probable sulfate-reduction as previously suggested (Heijs et al., 2008), until 22 cmbsf where it reached 12 mM. Below 22 cmbsf, the sulfate concentration gradually increased (Fig. 2). It has been shown that various electron acceptors, such as sulfate diffuse upwards from deep brines (D'Hondt et al., 2004; Parkes et al., 2005). Hence, the changing sulfate profile at Napoli could also be reasonably explained by a mixing of porewater sulfate with upwards diffusing sulfate-rich brine fluids. Methane was present in the Napoli sediments from about 60 to 130 cmbsf with a peak occurring at 130 cmbsf (Fig. 2). Acetate porewater concentrations were high and overall increased with depth, with 80 µM in near-surface sediments (Fig. 2) and maximum concentration at 85 cmbsf (448 µM), which overlapped with a broad peak in acetate methanogenesis rates. The acetate concentrations range (80-448 µM) were surprisingly high compared not only to seep and non-seep sediments (Newberry et al., 2004; Parkes et al., 2007), but also compared to brine impacted mud volcano sediments in the Gulf of Mexico (maximum 60 µM, Joye et al., 2009). Concentrations of dissolved inorganic carbon (measured as free CO_2) increased with depth to a maximum of 8.77 mM at 40 cmbsf (Supplementary Material. SM2), and then returned to shallow sediment concentrations.

Archaeal diversity and depth distribution.

The DGGE profiles for archaeal 16S rRNA genes (Fig. 3) of DNA from the centre of the Napoli mud volcano had 11 single major bands from 0 to 120 cmbsf depth. This highlights a very low archaeal diversity in these sediments. Sections 40-60 and 100-120 cmbsf had no visible bands. As ***mcrA*** genes were successfully amplified from these two sections, it is clear that the 16S archaeal primers that were used did not cover all methanogenic or methanotrophic sequences within the Napoli sediments, as mentioned elsewhere (Newberry et al., 2004). Band sequences NapK-dggeB1 to B3, and B5, B6 were affiliated to the methanotrophic ANME-1 group (with 96 to 99% similarity) in top sections 0-20 and 20-40 cmbsf (Table 1). Band sequences NapK-dggeB7 and B8 were affiliated with the ANME-2 with 98% similarity, and NapK-dggeB9 with the ANME-3 with 98% similarity in the 60-80 cmbsf section. Finally 2

band sequences Napk-dggeB4 at 0-20 cmbsf and B10 at 80-100 cmbsf were affiliated with clones of the Marine Benthic Group D (MBG-D) with 100 and 98% similarity to sequences from hypersaline sediments of the Gulf of Mexico (Lloyd et al., 2006). Selection of sediment samples for clone libraries of ***mcrA*** genes was based on the measured peaks in methanogenic activities (Fig. 2 and Supplementary Material. SM2), at depth sections 40-60, 60-80, and 100-120 cmbsf. A total of 42 ***mcrA*** sequences from sediment depths 40 to 60 cmbsf, 29 from depths 60 to 80 cmbsf, and 40 from depths 100 to 120 cmbsf were analyzed. Rarefaction curves generated for ***mcrA*** clones obtained from the 3 sections indicated saturation (Supplementary Material. SM3), while percent coverage was determined to be 87%, 73% and 71% for 40-60, 60-80 and 100-120 cmbsf respectively for the clone libraries. The ***mcrA*** phylotypes at 40 to 60 and 100 to 120 cmbsf were mainly affiliated with the ANME-1 (***mcrA*** group a/b, Fig. 4). Some sequences were also closely related to the ANME-2a (***mcrA*** group e) and with methylotrophic methanogens of the ***Methanococcoides*** (Fig. 4, Supplementary Material. SM4). In the 60 to 80 cmbsf sediment sections, all ***mcrA*** gene sequences were affiliated with the ANME-1 cluster probably involved in the anaerobic oxidation of methane (Fig. 4). ANME-1 sequences were detected in layers 20 to 40 cmbsf where methane concentrations were concave up, and below where sulfate removal was rapid, both typical of an AOM zone and consistent with the authigenic carbonate formation.

DGGE fingerprinting and ***mcrA*** clone library analysis showed that ANME-1 were present at all depths, except for the 80-100 cmbsf whereas the same analysis highlighted that ANME-2a were present from 40 to 120 cmbsf, with the same exception at 80-100 cmbsf. The ANME-2a subgroup was previously mostly detected in cold seep environment dominated by low fluid fluxes (Mills et al., 2003; Inagaki et al., 2004; Mills et al., 2004; Fang et al., 2006; Niemann et al., 2006), and also in hypersaline sediments in the Chefren mud volcano in the Nile Deep-Sea Fan (Omoregie et al., 2008).

The ***mcrA*** group a/b gene of the Napoli mud volcano formed one distinct cluster within the phylogenetic tree. This cluster contained sequences closely affiliated with ANME-1 genes from hypersaline sediments of the Gulf of Mexico with 94 to 97% of similarity. In their study, Lloyd ***et al.*** (2006) identified these ANME-1 as ANME-1b subcluster, and proposed that these ANME-1b could be a high salt adapted subpopulation surviving in an environment where other ANME groups could not.

Also, members of the ANME-1 group have been detected in other environments with high salinities such as a hydrothermal (45 °C) mud vent habitat underneath the deep-sea brine lake Urania in the Eastern Mediterranean (Yakimov et al., 2007a), the brine lake of the l'Atalante Basin (Yakimov et al., 2007b), and an Arctic hypersaline perennial spring (Niederberger et al., 2010).

Given the very high chloride concentrations in the Napoli sediment sections from which the clone libraries were constructed (i.e. 3000 mM at 40 cmbsf, and 4900 mM at 120 cmbsf) it is possible that the Napoli ***mcrA a/b*** sequences belong to the ANME-1 subcluster adapted to high salinity habitats. In the hypersaline sediments of a mud volcano in the Gulf of Mexico, there was no evidence for AOM, even though high methane fluxes were detected (Joye et al. 2009). In contrast, in the Napoli mud volcano sediments there was indirect evidence of AOM occuring in hypersaline sediments, where methane was also present.

Methanogenic activities.

Methanogenic activity using methylamine was the only significant pathway (Supplementary Material. SM2) in the shallow sediment layers (0 to 40 cmbsf) where sulfate concentrations were maximum and chloride concentrations were at the lowest values. Methylamine methanogenesis turnover rates were more than 10^2 times higher than those for methanol methanogenesis in these same layers. Methanol methanogenesis turnover rates were generally very low but a peak of activity occured at about 50 cm and in the methane-rich layers, and again at 90 cmbsf. Methane production was detected from the same depth interval in non hypersaline media designed to enrich methylotrophic and hydrogenotrophic methanogens (trimethylamine [TMA] and H_2/CO_2). Total DNA was extracted from 10^{-1} and 10^{-2} dilution series of the TMA enriched medium inoculated with the 0-20 cmbsf sediment section that produced methane. Phylogenetic affiliation of the 16S rRNA gene sequences NapK-0_20-enr35, and NapK-0_20-enr36 showed 99% sequence similarity with clone Tommo05_1274_3_Arch90 of the ***Euryarchaeota*** (FM179838) from the Tommeliten methane seep, in the North Sea (Wegener et al., 2008), and respectively 97% and 98% of sequence similarity with the closest cultured methylotrophic methanogen ***Methanococcoides methylutens*** (M59127). Clone NapK-80_100-enr37 obtained from the 10^{-1} dilution series of the TMA enriched medium of the 80-100 cmbsf section showed 99% sequence similarity with ***Methanococcoides***

171 ***methylutens*** (FJ477324). Finally clone Napk-0_20-enr74 from the 10^{-2} dilution series
172 of the H_2/CO_2 enriched medium at the 80-100 cmbsf section had a 95% sequence
173 similarity to the carbon dioxide reducing methanogen ***Methanogenium marinum***
174 (NR_028225). However, as enrichments were performed at seawater salinity and not
175 sediment porewater salinity, these methanogens may not represent the ***in situ***
176 halophilic methanogenic community.
177 Culture-dependent and -independent methods were successful in identifying
178 ***Methanococcoides*** related methanogens from 0 to 120 cmbsf. These methanogens
179 are obligate methylotrophs using only methanol and methylamines as substrates
180 (Garcia et al., 2000). The Sulfate Reducing Bacteria (SRB) outcompete methanogens
181 for substrates such as H_2 and acetate in sediments dominated by sulfate-reducing
182 process (Holmer et al., 1994). However, SRB do not compete for methylated
183 substrates that are known to be mostly present in near sediment surfaces (Cetecioglu
184 et al., 2009). Then methylotrophic methanogens are able to outcompete SRB in
185 sulfate-rich marine sediments (Purdy et al., 2003; Dhillon et al., 2005; Roussel et al.,
186 2009). Oremland ***et al***. (1982) reported that methanol and trimethylamines were
187 important substrates for methanogens in salt marsh sediments, dominance of
188 ***Methanoccoides***-type methanogens in sediments of Skan Bay (Kendall et al., 2007)
189 and in sediments of mangroves (Lyimo et al., 2000; Lyimo et al., 2009) were
190 previously reported. Methylamines were also shown to be the main methanogenic
191 catabolic substrate in the hypersaline brine of l'Atalante basin (McGenity, 2010). Pure
192 cutures of methylotrophic methanogens of the ***Methanohalophilus*** genus using non
193 competitive substrates such as methylated amines or methanol show higher
194 tolerances to high salinity, up to 24 to 25% NaCl (Oren, 1999). Methylotrophic
195 methanogens yields more free-energy (-191.1 kJ/mol of trimethylamine) than
196 acetoclastic (-31.1 kJ/mol of acetate) or hydrogenotroph (-131 kJ/mol of hydrogen)
197 probably allowing methylotrophic methanogens to maintain an osmotically balanced
198 and functional cytoplasm in hypersaline environments (Oren, 1999). Also, various
199 organic osmotic compounds were detected in halophilic methanogens such as
200 glycine betaine, glutamine, β-glutamate or N^{ε}-acetyl β-lysine (Oren, 1999). Zhilina ***et***
201 ***al***. (1990) discovered an halophilic homoacetogen in cyanobacterial mats of Sivash
202 (Crimea) that produces acetate and methylamines from betaine, which are potential
203 catabolic substrates for acetoclastic and methylotrophic methanogenesis.
204 The closest cultivated methylotrophic methanogen was ***Methanococcoides***

alaskense, a psychrophilic strain isolated from Skan Bay in Alaska, having an optimum temperature for growth at 23 °C (Singh et al., 2005). ***M. alaskense*** was also detected in a cold perennial spring of the Canadian high Arctic (Perreault et al., 2007). Cells of the type strain ***M. alaskense***, AK-5^T grew in range of Na^+ concentrations below that of seawater. Thus it seems that methylotrophic methanogens of the ***Methanococcoides*** are present and adapted for the moderate (14 °C) temperature and hypersaline sediments of the Napoli mud volcano. Both hydrogenotrophic and acetoclastic methanogenesis activities occured in sediment of the Napoli mud volcano but were generally low. Hydrogenotrophic methanogenesis was the dominant methane formation pathway below 50 cmbsf (Fig. 2), rates being 25 times higher (14 pmol cm^{-3} d^{-1}) than acetoclastic methanogenesis in the same sediment depth (e.g. 70 cmbsf). Considering competition with the SRB for substrates in the upper layers, it is not surprising to find hydrogenotrophic methanogenesis in the deeper methane-rich sediment layers. Low rates of acetate methanogenesis followed a similar depth trend to hydrogenotrophic methanogenesis with a peak at 70 cmbsf (0.6 pmol cm^{-3} day^{-1}). However, a second peak (0.25 pmol cm^{-3} day^{-1}) of activity occured at 125 cmbsf. This similar depth distribution of hydrogenotrophic and acetoclastic methanogenesis was previously reported in two brines from the northern Gulf of Mexico continental slope (Joye et al., 2009). Acetate methanogenesis rates in the Napoli mud volcano were in agreement with those measured in sediments of the Nankai Trough (maximum rate 0.11 pmol cm^{-3} day^{-1}) (Newberry et al., 2004). Interestingly, hydrogenotrophic methanogenesis rates were below activity rates measured in other marine sediments (Newberry et al., 2004; Parkes et al., 2007).

The presence of methanogenesis activities from hexadecane, a long chain alkane (Supplementary Material. SM2) around ~80 cmbsf demonstrated that methane production from satured hydrocarbons might be significant as previously shown in stable anaerobic enrichments (Zengler et al., 1999). Interestingly, maximum turnover of hexadecane to methane occured at a similar depth to peaks in both hydrogenotrophic and acetotrophic methanogenis rates. A syntrophic association involving methanogens and bacteria to degrade hexadecane to methane most likely would be involved (Dolfing et al., 2008), with acetogenic bacteria decomposing hexadecanes to acetate and H_2, which are in turn are available for acetoclastic and hydrogenotrophic methanogens. Grabowski ***et al***. (2005) observed in a low-temperature and low-salinity petroleum reservoir that homoacetogens were the

dominant cultivated organisms, and that methanogenesis was the dominant terminal process. Acetoclastic and hydrogenotrophic methanogenesis were surmised to be involved in the final step of hydrocarbon degradation in a petroleum hydrocarbon-contaminated aquifer (Kleikemper et al., 2005). Also, Lloyd ***et al***. (2006) detected sequences possibly related to methanogens in the petroleum-rich and hypersaline methane seep sediments of the Gulf of Mexico. Schulz ***et al***. (1997) showed that the sediments mobilized in the Napoli mud volcano were characterized by gaseous hydrocarbons, and that the sediments comprising the mud breccia originated from 4900 to 7500 mbsf. Hence, the Napoli mud volcano probably displays a wide range of substrates producing methane, including deep sourced petroleum.

Overall, PCR-DGGE and ***mcrA*** gene analysis demonstrated the presence of ANME-1, 2 and 3 clusters in sediments where hydrogenotrophic and acetoclastic methanogenesis rates were measured, suggesting that AOM is probably also present and active. CO_2 produced by anaerobic methane oxidation mediated by ANME, plus AOM metabolic intermediates could be available for the hydrogenotrophic methanogenesis thus enhancing methane production (Parkes et al., 2007). Sulfate-reducing bacteria can be inhibited by high salinities (Brandt et al. 2001), which may enable methanogens to occur even in the presence of high sulfate concentrations, as in the Napoli mud volcano sediments.

Below 100 cmbsf, acetoclastic methanogenesis was the dominant pathway for methane production. Hence, a shift from hydrogenotrophic to acetoclastic methanogenesis occured. Bicarbonate can also be converted to acetate by acetogens (Zepp Falz et al., 1999). Acetogens were found to be important competitors of hydrogenotrophic methanogens in a low-sulfate hypersaline microbial mat collected from salterns in Baja (Kelley et al., 2006). Also, halophilic homoacetogens were reported in cyanobacterial mats, capable of producing acetate from betaine, or bicarbonate (Zhilina et al., 1990). Even though the acetogenic reaction yields less energy than the actoclastic reaction, the halophilic homoacetogens of the order ***Haloanaerobiales*** have been shown to use an enegertically more efficient option to adapt to high salinity environments (Oren et al., 1999). Interestingly, acetate concentrations increased by ~80 cmbsf in Napoli porewaters (Fig. 2). Thus, the presence of halophilic homoacetogens below ~80 cmbsf could explain the absence of hydrogenotrophic methanogenesis, the increase

of acetate concentrations and the switch to acetoclastic methanogenesis in these sediment layers.

Influence of environmental factors on archaeal community composition in the Napoli sediments.

Sediments (down to 120 cmbsf depth) of the Napoli mud volcano center were characterized by very high chloride concentrations (from 1.5 M to 5 M), low stable temperatures, and presumably moderate fluid flows. Total prokaryotic cell numbers (Fig. 5) and percentage of dividing and divided cells were relatively low in the shallow sediments (1.49 x 10^8 cm^{-3} and 11% respectively), compared to the total prokaryotic depth distribution (Parkes et al., 2000). Microbial abundance strongly decreased with depth, reaching 5.5 x 10^6 cm^{-3} at 150 cmbsf. Only a limited number of prokaryotes can cope with the hypersaline conditions of the Napoli mud volcano sediments which explains the decrease in prokaryotic cell numbers with depth. However, within the upper overlap between sulfate and methane (~20 to 60 cmbsf, Fig. 2), there is a clear increase in total cell numbers above this decreasing trend (Fig. 5), which suggests active AOM (Parkes et al., 2005) and is consistent with the presence of ANME-1 sequences (Table 1).

Although microbial abundance generally decreased with increasing chloride concentrations, methanogenic activities in the centre of Napoli mud volcano (Charlou et al., 2003) were comparable to those measured in subsurface sediments (Webster et al., 2008), but lower than rates of methanogenesis in Mediterranean brines and Gulf of Mexico (Joye et al., 1999; van der Wielen et al., 2005; Daffonchio et al., 2006). This could be linked to the ascending fluid flows in the center of the mud volcano, that could hinder efficient methanogenesis. Three factors are known to influence methanogenic pathways: salinity, temperature and availability of substrates (Zepp Falz et al., 1999; Glissmann et al., 2004; McGenity, 2010). Salinity is a major factor in determining microbial community structure, and hypersaline sediments can be phylogenetically more diverse than other environments (Lozupone et al., 2007). However, saline gradients are composed of a number of electron acceptors, donors, nutrients, and carbon sources available for the microorganisms (McGenity, 2010). In addition, salinity may indirectly control substrate availablity for methanogens, by controling the diversity of organisms producing their substrates (***i.e.***, halophilic acetogens and fermenters producing acetate and methylamines). Traditionally, high

salinity is thought to favour hydrogenotrophic and methylotrophic methanogenesis, because acetoclastic methanogens cannot tolerate these extrême halophilic conditions (>60 ‰ salinity) (Oren, 1999). However, acetoclastic methanogenesis does occur in Napoli sediments, and at depths where chloride concentrations are higher than 4 M (>140 ‰). Acetoclastic methanogenesis at a salinity exceeding 60‰ has already been reported in brine sediments of a mud volcano in the Gulf of Mexico (Joye et al., 2009), demonstrating that some acetoclastic methanogens have adapted to high salinity environments. In contrast, uncutivated archaeal sequences affiliated with the MBG-D have been detected in many saline and hypersaline environments (Benlloch et al., 2002; Sorensen et al., 2005; Lloyd et al., 2006; Jiang et al., 2008; Omoregie et al., 2008). Jiang et al. (2008) propose that high salinity and alkalinity, among other unknown factors, could play an important role in controlling the distribution of marine benthic groups, such as the MBG-D. Hence the hypersaline regime in the Napoli center sediments could have influenced establishment of these MBG-D populations.

Studies conducted on lake sediments show that a shift from 4 to 20°C induces a shift from acetoclastic to hydrogenotrophic methanogenesis (Zepp Falz et al., 1999; Glissmann et al., 2004). Indeed Schulz ***et al***. (1997) hypothesize that in lake sediments at low temperatures, hydrogenotrophic methanogens are limited by the lack of supply of H_2, which is linked with the idea that H_2-producing syntrophs are sensitive to low temperatures. In the Napoli sediments, the temperature at 70 cmbsf was around 14 °C which could be one factor explaining why overall hydrogenotrophic methanogenesis is higher than acetoclastic methanogenesis. In this context, Napoli sediments are similar to other marine sediments as these are also dominated by hydrogenotrophic methanogenesis (Whiticar et al., 1986).

Therefore, the brine affected Napoli mud volcano in the Mediterranean Sea represents a dynamic ecological niche for methanogens and other prokaryotes that have to adapt to variations in fluid flow and composition, and high salinity.

EXPERIMENTAL PROCEDURES

Site description and sediment sampling.

Sediment cores were collected from the center of the Napoli mud volcano at 1940 metres of water depth (Fig. 1) in the Eastern Mediterranean Sea, during the Ifremer MEDECO cruise with the research vessel Pourquoi Pas? in October/November 2007.

Two gravity cores KUL-3 (33°43.497'N, 24°41.1648'E) and KUL-4 (33°43.508'N, 24°41.1549'E), 160 cm and 120 cm in length, respectively, were obtained. Temperature gradients were measured using sensors attached to the gravity cores. Immediately after retrieval, the KUL-3 and KUL-4 cores were sectioned aseptically in 20-cm-thick layers in a cold room (4°C), and mini-cores of sediment were removed for gas and molecular analysis. Samples for molecular analysis were collected by using cut-off sterile 5 mL syringes in the 20 cm sediment sections of KUL-4 and were frozen at –80°C for nucleic acid extractions. For the KUL-3 core, 20 cm sections were flushed with nitrogen, hermetically sealed in aluminium bag-rolls (Grüber-Folien, Germany), and transported to the laboratory at 4°C for subsequent methanogenesis rate measurements and pore water analysis.

Biochemistry.

Porewater was obtained by centrifuging approximately 10 g of sediment for 15 minutes at 3000 x g at 4 °C. The porewater was then stored at -20 °C until required. Depth distribution of dissolved cations were quantified from diluted and filtrated porewater by using ion exchange chromatography, as described below. Cation concentrations were measured using an isocratic DX120 ion chromatography system (DIONEX Corporation, Sunnyvale, CA) fitted with Ionpac CS 12A columns and a supressor (CSRS-ultra II) unit in combination with a DS4-1 heated conductivity cell. Components were separated using a methasulfonic acid (18 mM) gradient, with a flow of 1 mL min^{-1}.

Pore water sulfate and acetate concentrations were measured by ion exchange chromatography using an ICS-2000 ion chromatography system (Dionex®, UK) fitted with two AS15-HC 4 mm columns inseries, and a Dionex® Anion Self-Regenerating Suppressor(ASRS®-ULTRA II 4-mm) unit in combination with a Dionex®DS6 heated conductivity cell. Components were separated using a potassium hydroxide gradient program as follows: 6.0 mM KOH (38 min isocratic), 16.0 mM KOH min-1 to 70 mM (17 min isocratic).

Methane concentrations were determined from 3 cm^3 sediment sample sealed in glass tubes containing 6 mL NaOH (2.5% w/v), on board using the headspace technique coupled with a gas chromatograph GC (HSS-GC) equipped with a thermal-conductivity detector (TCD) and a flame-ionisation detector (error of 4%). Helium was the carrier gas, and column temperature was 40 °C (details in Sarradin et al., 1996).

Methanogenesis rate measurements.

Radiotracer experiments using ^{14}C labelled substrates were conducted in the laboratory at Cardiff University, UK according to Parkes et al. (2007) using the 4°C stored cores. Intact 5 mL syringe subcores were taken in the center of core, and sealed with sterile Suba Seals (Sigma-Aldrich, Missouri, USA). These samples were separately injected with radiotracers ([^{14}C]bicarbonate, [^{14}C]acetate, [^{14}C]methanol [^{14}C]methylamine or [^{14}C]hexadecane) and incubated at close to ***in situ*** temperatures (15°C). Activity was then stopped by freezing before processing in the laboratory. Methane production rates were calculated based on the proportion of labelled gas produced from the ^{14}C-substrate, and the measured porewater substrate concentration adjusted for sediment porosity and incubation time ([^{14}C]acetate, methanol and methylamine – 15-20 h; [^{14}C]bicarbonate and hexadecane – 40-46 h). Methanol, methylamine and hexadecane methanogenic rates were expressed as turnover rates as their porewater concentrations were unknown. Because incubation conditions were not identical to conditions in the original sediment, measured rates might differ from those ***in situ***.

Acridine Orange Direct Counts

Total prokaryote numbers were determined by AODC counts as previously described (Parkes et al., 2005). Trends and peaks in rate and AODC data were assessed by analysis of variance, the sum of squares simultaneous test procedure and the Moodmedian test, as appropriate using Mini-Tab 14.2.

Culture media for enrichment of methanogens.

One volume of sediment subsample (10 cm^3) was transferred into an anaerobic cabinet and then into 50 mL vials containing one volume (10 mL) of sterile and reduced Artificial Sea Water (ASW). ASW corresponded to medium 141 of DSMZ devoid of organic carbon substrates. The sediment slurries were further reduced with Na_2S if necessary and stored at 4°C until processing. Enrichment were performed anaerobically in 50 mL vials according to Balch and Wolfe (1976). Medium 141 from the DSMZ was used with slight modifications : organic substrates were omitted except yeast extract which was adjusted to 0.2 g L^{-1}. The medium was prepared and

sterilized under 80 N_2 and 20% CO_2 gas atmosphere. In order to enrich CO_2-reducing, aceticlastic and methylotrophic methanogens, three enrichment media supplemented with H_2 (200 kPa), acetate (10 mM), trimethylamine (TMA, 20 mM) were used. One gram of sediment from the different sections of the KUL-4 core were inoculated into 9 mL of medium (pH 7). The suspension was mixed and serially diluted until 10^{-3}. The enrichments were incubated at close to ***in situ*** temperature of 15°C. Cultures were periodically checked for methane production for one year. The methane detection was performed directly in the headspace of vial cultures by a micro MTI M200 Gas Chromatograph equipped with MS-5A capillary column and Poraplot U capillary column. Positive enrichment dilutions of methanogens were monitored by microscopic observation under UV-light and PCR-DGGE. For dilutions showing one DGGE band, 16S rRNA genes were amplified using the A8F and A1492R primers (Casamayor et al., 2000), cloned and sequenced as subsequently described.

DNA extraction and purification.

Total genomic DNA was directly extracted and purified from 5 g of wet sediment for all 20-cm-thick sections in duplicates, by using the Zhou ***et al.*** (1996) method with modifications. Sediment samples were mixed with DNA extraction buffer as described by Zhou ***et al.***, and then frozen in liquid N_2 and thawed at 65°C 3 times. The pellet of crude nucleic acids obtained after centrifugation, was washed with cold 80% ethanol, and resuspended in sterile deionized water, to give a final volume of 100 µL. Crude DNA extracts were then purified using the Wizard DNA clean-up kit (Promega, Madison, WI). DNA extracts were aliquoted and stored at -20 °C until required for PCR amplification.

PCR-DGGE amplification of total DNA.

Archaeal 16S rRNA genes were amplified by PCR from purified DNA extracts using the Archaeal targeted primers pair 8F (5'-CGGTTGATCCTGCCGGA-3') and 1492R (5'-GGCTACCTTGTTACGACTT-3') (Casamayor et al., 2000). All PCR reactions (total volume reaction 25 µL) contained 1 µL purified DNA template (1/25 dilution), 1 X PCR buffer (Promega, Madison, WI), 2 mM $MgCl_2$, 0.2 mM of each dNTP, 0.4 mM of each primer (Eurogentec) and 0.6 U Go***Taq*** DNA polymerase (Promega, Madison, WI). Amplification was carried out using the GeneAmp PCR 9700 System (Applied

Biosystems, Foster City, CA). The PCR conditions were as follows: denaturation at 94°C for 1 min, annealing at 49°C for 1 min 30 s, and extension at 72°C for 2 min for 30 cycles. All the archaeal 16S rRNA gene PCR products were then re-amplified with primers 340F (5'-CCCTACGGGGYGCASCAG-3') (Vetriani et al., 1999) containing a GC clamp (5'-CGCCCGCCGCGCCCCGCGCCCGTCCCGCCGCCCCCGCCCG-3') at the 5' end and 519R (5'-TTACCGCGGCKGCTG-3') (Ovreas et al., 1997). The PCR conditions were as follows: denaturation at 94°C for 30 s, annealing at 72°C to 62°C (touchdown -0.5°C.cycle^{-1}) for 30 s, and extension at 72°C for 1 min, for 20 cycles, then denaturation at 94°C for 30 s, annealing at 62°C for 30 s, and extension at 72°C for 1 min, for 10 cycles, final extension at 72°C for 30 min (Janse et al., 2004).

To restrict contamination to a minimum, PCR experiments was carried out under aseptic conditions (Captair® bio, Erlab, Fisher Bioblock Scientific) using autoclaved and UV-treated plasticware and pipettes, and only sterile nuclease-free molecular grade water (MP Biomedicals, Solon, OH, USA). Positive (DNA extracted from pure cultures) and negative (molecular grade water) controls were used in all PCR amplifications.

DGGE fingerprinting analysis, band excision and sequencing.

DGGE was carried out as described by Webster et al. (2003) with some modifications. PCR products were separated by DGGE using the D-Gene™ System (Bio-Rad Laboratories, Hercules, CA) on 8% (w/v) polyacrylamide gels (40% acrylamide/bis solution 37.5:1 Bio-Rad) with a linear gradient of urea and formamide between 20% and 60% (100% denaturing conditions are defined as 7M urea and 40% (v/v) formamide). Gels were poured with the aid of a 30 mL volume Gradient Mixer (Hoefer SG30, GE Healthcare, Buckinghamshire, UK) and prepared with 1 X TAE buffer (MP Biomedicals, Solon, OH, USA). Electrophoresis was carried out at 60°C, 200 V for 5 hours (with an initial electrophoresis for 10 min at 80 V) in 1 X TAE buffer. Polyacrylamide gels were stained with SYBRGold nucleic acid gel stain (Invitrogen, San Diega, CA) for 30 min, and viewed using the Typhoon 9400 Variable Mode Imager (GE Healthcare, Buckinghamshire, UK). Individual DGGE bands of interest were excised and washed in sterile-nuclease free molecular grade water for 10 min. Bands were then air-dried and crushed in 10-20 µL molecular grade water and incubated overnight at 4°C. The supernatent (1µL) was used as template DNA in

a nested PCR using primer set 340F and 519R. The PCR products of excised DGGE bands were sequenced with primer 519R, using an ABI PRISM 3100-Genetic Analyzer (Applied Biosystems, Foster City, CA) at the Biogenouest® plateform of Roscoff Marine laboratory (France).

mcrA PCR amplification, and cloning.

Genes coding for the alpha subunit of the methyl- coenzyme M-reductase's (***mcrA***) were amplified using the ME1 (5'-GCMATGCARATHGGWATGTC-3') and ME2 (5'-TCATKGCRTAGTTDGGRTAGT-3') primers (Hales et al., 1996). The PCR conditions were as follows: denaturation at 94°C for 40 s, annealing at 50°C for 1 min 30 s, and extension at 72°C for 3 min for 30 cycles. PCR products were purified with the QIAquick Gel Extraction kit (QIAGEN, Hilden, Germany) and analyzed on 1% (w/v) agarose gels run in 1 X TAE buffer stained with ethidium bromide and then UV-illuminated. Purified PCR products were cloned into TOPO® XL PCR Cloning Kit, and transformed into ***Escherichia coli*** TOP10 One Shot® cells (Invitrogen, San Diego, CA) according to the manufacturer's recommendations.

DNA sequencing and phylogenetic analysis.

16S rRNA and ***mcrA*** gene sequences were obtained using BigDye terminator chemistry and determined on a ABI PRISM 3100-Genetic Analyzer automated capillary sequencer (Applied Biosystems, Foster City, CA). Cloned 16S rDNA and ***mcrA*** gene fragments were sequenced using the M13 reverse primer (5'-CAGGAAACAGCTATGAC-3') universal primer and analyzed using the NCBI BLASTN search program within GeneBank (http://blast.ncbi.nlm.nih.gov/Blast) (Altschul et al., 1990). The presence of chimeric sequences in the clone libraries was determined with the CHIMERA CHECK program of the Ribosomal Database Project II (Center for Microbial Ecology, Michigan State University, http://wdcm.nig.ac.jp/RDP/html/analyses.html). Potential chimeras were eliminated before phylogenetic trees were constructed. The ***mcrA*** sequences were then edited in the BioEdit v7.0.5 program (Hall, 1999), translated into amino acid sequences, and aligned using ClustalX (Larkin et al., 2007). Sequence data was analysed with the MEGA4.0.2 program (Tamura et al., 2007). The phylogenetic trees were calculated by the neighbour-joining analysis. The robustness of inferred topology was tested by boostrap resampling (1000).

Rarefaction curves were calculated for each ***mcrA*** clone library using the RarFac program (http://www.icbm.de/pmbio/), and we used a 97% similarity level to define the groups of sequences. Libraries' coverage was calculated using the following formula: $C=[1-(n_1/N)]*100$, where n_1 is the number of unique OTUs, and N is number of clones in the library (Singleton et al., 2001).

Nucleotide sequence accession numbers.

The sequence data reported here will appear in GenBank nucleotide sequence databases under the accession no. HM004960 to HM005070 for ***mcrA*** genes and HM004950 to HM004959 for 16S rRNA gene DGGE band sequences. Sequences obtained from enrichments are no. HM004946 to HM004949.

Acknowledgements.

We would like to thank Josée Sarrazin, the chief scientist of the MEDECO cruise, the ROV team, the officers and crew of the RV ***Pourquoi Pas?*** as well as the shipboard scientific community for their help at sea. This work was funded by the HERMES project Contract No: GOCE-CT-2005-511234-1, the ANR Deep Oases, and NERC, UK (NE/F018983/1).

REFERENCES

Altschul, S.F., Gish, W., Miller, W., Myers, EW, and Lipman D.J. (1990) Basic local alignment search tool. J Mol Biol 215: 403-410.

Aloisi, G., Pierre, C., Rouchy, J.-M., Foucher, J.-P., and Woodside, J. (2000) Methane-related authigenic carbonates of eastern Mediterranean Sea mud volcanoes and their possible relation to gas hydrate destabilisation. Earth Planet Sci Lett 184**:**321-338.

Balch, W.E., and Wolfe, R.S. (1976) New approach to the cultivation of methanogenic bacteria: 2-mercaptoethanesulfonic acid (HS-CoM)-dependent growth of Methanobacterium ruminatium in a pressurized atmosphere. Appl Environ Microbiol 32: 781-791.

Benlloch, S., López-López, A., Casamayor, E.O., Ovreas, L., Goddard, V., Daee F.L., et al. (2002) Prokaryotic genetic diversity throughout the salinity gradient of a coastal solar saltern. Environ Microbiol 4: 349-360.

Boetius, A., Ravenschlag, K., Schubert, C.J., Rickert, D., Widdel, F., Gieske, A., et al. (2000) A marine microbial consortium apparently mediating anaerobic oxidation of methane. Nature 407: 623-626.

Brandt, K.K., Vester, F., Jensen, A.N., and Ingvorsen, K. (2001) Sulfate reduction dynamics and enumeration of sulfate-reducing bacteria in hypersaline sediments of the Great Salt Lake (Utah, USA). Microb Ecol 41:1-11.

Casamayor, E.O., Schäfer, H., Baneras, L., Salio, C.P., and Muyzer, G. (2000) Identification of and Spatio-Temporal Differences between Microbial Assemblages from Two Neighboring Sulfurous Lakes: Comparison by Microscopy and Denaturing Gradient Gel Electrophoresis. Appl Environ Microbiol 66: 499-508.

Cetecioglu, Z., Ince, B.K., Kolukirik, M., and Ince, O. (2009) Biogeographical distribution and diversity of bacterial and archaeal communities within highly polluted anoxic marine sediments from the marmara sea. Marine Pollution Bulletin 58: 384–395.

Chaduteau, C. (2008) Origin and circulation of fluids in sediments of margins, Contribution of Helium and methane to the comprehension of the processes, Study of two zones. PhD thesis. Université de Bretagne Occidentale, France. p.121.

Charlou, J.L., Donval, J.P., Zitter, T., Roy, N., Jean-Baptiste, P., Foucher, J.P., et al. (2003) Evidence of methane venting and geochemistry of brines on mud volcanoes of the eastern Mediterranean Sea. Deep-sea research Part I 50: 941-958.

D'Hondt, S., Jørgensen, B.B., Miller, D.J., Batzke, A., Blake, R., Cragg, B.A., et al. (2004) Distributions of Microbial Activities in Deep Subseafloor Sediments. Science 306: 2216-2221.

Daffonchio, D., Borin, S., Brusa, T., Brusetti, L., van der Wielen, P.W.J.J., Bolhuis, H., et al. (2006) Stratified prokaryote network in the oxic–anoxic transition of a deep-sea halocline. Nature 440: 203-207.

Dhillon, A., Lever, M., Llyod, K.G., Albert, D.B., Sogin, M.L., and Teske, A. (2005) Methanogen diversity evidenced by molecular characterization of methyl coenzyme M reductase A (mcrA) genes in hydrothermal sediments of the Guyamas basin. Appl Environ Microbiol 71: 4592-4601.

Dimitrov, L.I. (2003) Mud volcanoes-a significant source of atmospheric methane. Geo-Marine Letters 23: 155-161.

Dolfing, J., Larter, S.R., and Head, I.M. (2008) Thermodynamic constraints on methanogenic crude oil biodegradation. ISME J 2: 442–452.

Fang, J., Shizuka, A., Kato, C., and Schouten, S. (2006) Microbial diversity of cold-seep sediments in Sagami Bay, Japan, as determined by 16S rRNA gene and lipid analysis. FEMS Microbiol Ecol 57: 429-441.

Feseker, T., Dählmann, A., Foucher, J.-P., and Harmegnies, F. (2009) In-situ sediment temperature measurements and geochemical porewater data suggest highly dynamic fluid flow at Isis mud volcano, eastern Mediterranean Sea. Mar Geol 261: 128–137.

Garcia, J.-L., Patel, B.K.C., and Ollivier, B. (2000) Taxonomic, phylogenetic, and ecological diversity of methanogenic Archaea. Anaerobe 6: 205-226.

Glissmann, K., Chin, K.-J., Casper, P., and Conrad, R. (2004) Methanogenic Pathway and Archaeal Community Structure in the Sediment of Eutrophic Lake Dagow: Effect of Temperature. Microb Ecol 48: 389-399.

Grabowski, A., Nercessian, O., Fayolle, F., Blanchet, D., and Jeanthon, C. (2005) Microbial diversity in production waters of a low-temperature biodegraded oil reservoir. FEMS Microbiol Ecol 54: 427-443.

Haese, R.R., Hensen, C., and de Lange, G.J. (2006) Pore water geochemistry of eastern Mediterranean mud volcanoes: Implications for fluid transport and fluid origin. Mar Geol 225: 191- 208.

Hales, B.A., Edwards, C., Titchie, D.A., Hall, G., Pickup, R.W., and Sauders, J.R. (1996) Isolation and identification of methanogen-specific DNA from blanket bog peat by PCR amplification and sequence analysis. Appl Environ Microbiol 62.

Hall, T.A. (1999) BioEdit: a user-friendly biological sequence alignment editor and analysis program for Windows 95/98/NT. Nucleic Acids Symp Ser 41: 95–98.

Heijs, S.K., Laverman, A.M., Forney, L.J., Hardoim, P.R., and van Elsas, J.D. (2008) Comparison of deep-sea sediment microbial communities in the Eastern Mediterranean. FEMS Microbiol Ecol 64: 362-377.

Holmer, M., and Kristensen, E. (1994) Coexistence of sulfate reduction and methane production in an organic-rich sediment. Mar Ecol Prog Ser 107: 177-184.

Inagaki, F., Tsunogai, U., Suzuki, M., Kosaka, A., Machiyama, H., Takai, K., et al. (2004) Characterization of C1-metabolizing prokaryotic communities in methane seep habitats at the Kuroshima Knoll, southern Ryukyu Arc, by analyzing pmoA, mmoX, mxaF, mcrA, and 16S rRNA genes. Appl Environ Microbiol 70: 7445-7455.

Janse, I., Bok, J., and Zwart, G. (2004) A simple remedy against artifactual double bands in denaturing gradient gel electrophoresis. J Microbiol Methods 57: 279– 281.

Jiang, H, Dong, H., Yu, B., Ye, Q., Shen, J., Rowe, H., and Zhang, C. (2008) Dominance of putative marine benthic Archaea in Qinghai Lake, north-western China. Environ Microbiol 10: 2355–2367.

Joye, S.B., Connell, T.L., Miller, L.G., Oremland, R.S., and Jellison, R.S. (1999) Oxidation of ammonia and methane in an alkaline, saline lake. Limnol Oceanogr 44: 178-188.

644

645 Joye, S.B., Samarkin, V.A., Orcutt, B.N., MacDonald, I.R., Hinrichs, K.-U., Elvert, M.,
646 et al. (2009) Metabolic variability in seafloor brines revealed by carbon and sulphur
647 dynamics. Nature Geoscience 2: 349-354.

648

649 Kelley, C.A., Prufert-Bebout, L.E., and Bebout, B.M. (2006) Changes in carbon
650 cycling ascertained by stable isotopic analyses in a hypersaline microbial mat.
651 Journal of geophysical research 111: doi:10.1029/2006JG000212.

652

653 Kendall, M.M., and Boone, D.R. (2006) Cultivation of methanogens from shallow
654 marine sediments at Hydrate ridge, Oregon. Archaea 2: 1-8.

655

656 Kendall, M.M., Wardlaw, G.D., Tang, C.F., Bonin, A.S., Liu, Y., and Valentine, D.L.
657 (2007) Diversity of Archaea in marine sediments from Skan Bay, Alaska, including
658 cultivated methanogens, and description of Methanogenium boonei sp. nov. Appl
659 Environ Microbiol 73: 407-414.

660

661 Kleikemper, J., Pombo, S.A., Schroth, M.H., Sigler, W.V., Pesaro, M., and Zeyer, J.
662 (2005) Activity and diversity of methanogens in a petroleum hydrocarbon-
663 contaminated aquifer. Appl Environ Microbiol 71: 149-158.

664

665 Knittel, K., Lösekann, T., Boetius, A., Kort, R., and Amann, R. (2005) Diversity and
666 distribution of methanotrophic Archaea at cold seeps. Appl Environ Microbiol 71: 467-
667 479.

668

669 Knittel, K., and Boetius, A. (2009) Anaerobic Oxidation of Methane: Progress with an
670 Unknown Process. Annu Rev Microbiol 63: 311–334.

671

672 Kvenvolden, K.A. (1988) Methane hydrates-A major reservoir of carbon in the
673 shallow geosphere ? Chem Geol 71: 41-51.

674

675 Larkin, M.A., Blackshields, G., Brown, N.P., Chenna, R., McGettigan, P.A.,
676 McWilliam, H., et al. (2007) Clustal W and Clustal X version 2.0. Bioinformatics 23:
677 2947-2948.

Lloyd, K.G., Lapham, L., and Teske, A. (2006) An anaerobic methane-oxidizing community of ANME-1b Archaea in hypersaline Gulf of Mexico sediments. Appl Environ Microbiol 72: 7218-7230.

Lösekann, T., Knittel, K., Nadalig, T., Fuchs, B., Niemann, H., Boetius, A., and Amann, R. (2007) Diversity and abundance of aerobic and anaerobic methane oxidizers at the Haakon Mosby Mud Volcano, Barents Sea. Appl Environ Microbiol 73: 3348-3362.

Lozupone, C.A., and Knight, R. (2007) Global patterns in bacterial diversity. Proc Natl Acad Sci U S A 104: 11436–11440.

Lyimo, T.J., Pol, A., Op den Camp, H.J.M., Harhangi, H.R., and Vogels, G.D. (2000) Methanosarcina semesiae sp. nov., a dimethylsulfide-utilizing methanogen from mangrove sediment. Int J Syst Evol Microbiol 50: 171–178.

Lyimo, T.J., Pol, A., Jetten, M.S.M., and Op den Camp, H.J.M. (2009) Diversity of methanogenic archaea in a mangrove sediment and isolation of a new Methanococcoides strain. FEMS Microbiol Ecol 291: 247–253.

McGenity, T.J. (2010) Methanogens and Methanogenesis in Hypersaline Environments. In Handbook of Hydrocarbon and Lipid Microbiology, Part 8. Timmis, K.N. (ed). Springer-Verlag Berlin and Heidelberg, pp. 665-680.

Mikucki, J.A., Liu, Y., Delwiche, M., Colwell, F.S., and Boone, D.R. (2003) Isolation of a methanogen from deep marine sediments that contain methane hydrates, and description of Methanoculleus submarinus sp. nov. Appl Environ Microbiol 69: 3311-3316.

Milkov, A. (2000) Worldwide distribution of submarine mud volcanoes and associated gas hydrates. Mar Geol 167: 29-42.

Mills, H.J., Hodges, C., Wilson, K., MacDonald, I.R., and Sobecky, P.A. (2003) Microbial diversity in sediments associated with surface-breaching gas hydrate mounds in the Gulf of Mexico. FEMS Microbiol Ecol 46: 39-52.

Mills, H.J., Martinez, R.J., Story, S., and Sobecky, P.A. (2004) Identification of members of the metabolically active microbial populations associated with Beggiatoa species mat communities form Gulf of Mexico cold-seep sediments. Appl Environ Microbiol 70: 5447-5458.

Newberry, C.J., Webster, G., Cragg, B.A., Parkes, R.J., Weightman, A.J., and Fry, J.C. (2004) Diversity of prokaryotes and methanogenesis in deep subsurface sediments from the Nankai Trough, Ocean Drilling Program Leg 190. Environ Microbiol 6: 274-287.

Niederberger, T.D., Perreault, N.N., Tille, S., Lollar, B.S., Lacrampe-Couloume, G., Andersen, D. et al. (2010) Microbial characterization of a subzero, hypersaline methane seep in the Canadian High Arctic. ISME J 4: 1326–1339.

Niemann, H., Duarte, J., Hensen, C., Omoregie, E., Magalhaes, V.H., Elvert, M., et al. (2006) Microbial methane turnover at mud volcanoes of the Gulf of Cadiz. Geochim Cosmochim Acta 70: 5336-5355.

Olu-Le Roy, K., Sibuet, M., Fiala-Médioni, A., Gofas, S., Salas, C., Mariotti, A., et al. (2004) Cold seep communities in the deep eastern Mediterranean Sea: composition, symbiosis and spatial distribution on mud volcanoes. Deep-sea research Part I 51: 1915-1936.

Omoregie, E.O., Mastalerz, V., de Lange, G., Straub, K.L., Kappler, A., Røy, H., et al. (2008) Biogeochemistry and Community Composition of Iron- and Sulfur-Precipitating Microbial Mats at the Chefren Mud Volcano (Nile Deep Sea Fan, Eastern Mediterranean). Appl Environ Microbiol 74: 3198-3215.

Oremland, R.S., Marsh, L.M., and Polcin, S. (1982) Methane production and simultaneous sulphate reduction in anoxic, salt marsh sediments. Nature 296: 143-145.

Oren, A. (1999) Bioenergetic Aspects of Halophilism. Microbiology and Molecular Biology Reviews 63: 334–348.

Ovreas, L., Forney, L., Daae, F.L., and Torsvik, V. (1997) Distribution of bacterioplankton in meromictic Lake Saelenvannet, as determined by denaturing gradient gel electrophoresis of PCR-amplified gene fragmetns coding for 16S rRNA. Appl Environ Microbiol 63: 3367-3373.

Parkes, R.J., Cragg, B.A., and Wellsbury, P. (2000) Recent studies on bacterial populations and processes in subseafloor sediments: A review. Hydrogeology journal 8: 11-28.

Parkes, R.J., Webster, G., Cragg, B.A., Weightman, A.J., Newberry, C.J., Ferdelman, T.G., et al. (2005) Deep sub-seafloor prokaryotes stimulated at interfaces aver geological times. Nature 436: 390-394.

Parkes, R.J., Cragg, B.A., Banning, N., Brock, F., Webster, G., Fry, J.C., et al. (2007) Biogeochemistry and biodiversity of methane cycling in subsurface marine sediments (Skagerrak, Denmark). Environ Microbiol 9: 1146-1161.

Perreault, N.N., Andersen, D.T., Pollard, W.H., Greer, C.W., and Whyte, L.G. (2007) Characterization of the Prokaryotic Diversity in Cold Saline Perennial Springs of the Canadian High Arctic. Appl Environ Microbiol 73: 1532-1543.

Purdy, K.J., Munson, M.A., Cresswell-Maynard, T., Nedwell, D.B., and Embley, T.M. (2003) Use of 16S rRNA-targeted oligonucleotide probes to investigate function and phylogeny of sulphate-reducing bacteria and methanogenic archaea in a UK estuary. FEMS Microbiol Ecol 44: 361-371.

776 Roussel, E.G., Sauvadet, A.-L., Allard, J., Chaduteau, C., Richard, P., Cambon
777 Bonavita, M.-A., and Chaumillon, E. (2009) Archaeal Methane Cycling Communities
778 Associated with Gassy Subsurface Sediments of Marennes-Oléron Bay (France).
779 Geomicrobiol J 26: 31–43.
780
781 Sarradin, P.-M., and Caprais, J.C. (1996) Analysis of dissolved gases by headspace
782 sampling, gas chromatography with columns and detectors commutation. Preliminary
783 results. Analytical Communications 33: 371-373.
784
785 Schulz, S., Matsuyama, H., and Conrad, R. (1997) Temperature dependence of
786 methane production from different precursors in a profundal sediment (Lake
787 Constance). FEMS Microbiol Ecol 22: 207-213.
788
789 Shlimon, A.G., Friedrich, M.W., Niemann, H., Ramsing, N.B., and Finster, K. (2004)
790 Methanobacterium aarhusense sp nov., a novel methanogen isolated from a marine
791 sediment (Aarhus Bay, Denmark). Int J Syst Evol Microbiol 54: 759-763.
792
793 Singh, N., Kendall, M.M., Liu, Y., and Boone, D.R. (2005) Isolation and
794 characterization of methylotrophic methanogens from anoxic marine sediments in
795 Skan Bay, Alaska: description of Methanococcoides alaskense sp. nov., and
796 emended description of Methanosacina baltica. Int J Syst Evol Microbiol 55: 2531-
797 2538.
798
799 Singleton, D.R., Furlong, M.A., Rathbun, S.L., and Whitman, W.B. (2001)
800 Quantitative Comparisons of 16S rRNA Gene Sequence Libraries from
801 Environmental Samples. Appl Environ Microbiol 67: 4374–4376.
802
803 Sorensen, K.B., Canfield, D.E., Teske, A.P., and Oren, A. (2005) Community
804 Composition of a Hypersaline Endoevaporitic Microbial Mat. Appl Environ Microbiol
805 70: 7352–7365.
806
807 Sowers, K.R., and Ferry, J.G. (1983) Isolation and characterization of a
808 methylotrophic marine methanogen, Methanococcoides methylutens gen. nov., sp.
809 nov. Appl Environ Microbiol 45: 684-690.

Sowers, K.R., Baron, S.F., and Ferry, J.G. (1984) Methanosarcina acetivorans sp. nov., an acetoclastic methane-producing bacterium isolated from marine sediments. Appl Environ Microbiol 47: 971-978.

Tamura, K., Dudley, J., Nei, M., and Kumar, S. (2007) MEGA4: Molecular Evolutionary Genetics Analysis (MEGA) Software Version 4.0. Mol Biol Evol 24: :1596–1599.

van der Wielen, P.W.J.J., Bolhuis, H., Borin, S., Daffonchio, D., Corselli, C., Giuliano, L., et al. (2005) The Enigma of Prokaryotic Life in Deep Hypersaline Anoxic Basins. Science 307: 121-123.

von Klein, D., Arab, H., Völker, H., and Thomm, M. (2002) Methanosarcina baltica, sp. nov., a novel methanogen isolated from the Gotland Deep of the Baltic sea. Extremophiles 6: 103-110.

Vetriani, C., Jannasch, H.W., MacGregor, B.J., Stahl, D.A., and Reysenbach, A.-L. (1999) Population structure and phylogenetic characterization of marine bentic Archaea in deep-sea sediments. Appl Environ Microbiol 65: 4375-4384.

Webster, G., Newberry, C.J., Fry, J.C., and Weightman, A.J. (2003) Assessment of bacterial community structure in the deep sub-seafloor biosphere by 16S rDNA-based techniques: a cautionary tale. Journal of microbiological methods 55: 155-164.

Webster, G., Blazejak, A., Cragg, B.A., Schippers, A., Sass, H., Rinna, J., et al. (2008) Subsurface microbiology and biogeochemistry of a deep, cold-water carbonate mound from the Porcupine Seabight (IODP Expedition 307). Environ Microbiol.

Wegener, G., Niemann, H., Elvert, M., Hinrichs, K.-U., and Boetius, A. (2008) Assimilation of methane and inorganic carbon by microbial communities mediating the anaerobic oxidation of methane. Environ Microbiol 10:2287-2298.

Whiticar, M.J., Faber, E., and Schoell, M. (1986) Biogenic methane formation in marine and freshwater environments: CO2 reduction vs acetate fermentation-Isotope evidence. Geochim Cosmochim Acta 50:693-709.

Yakimov, M.M., Giuliano, L., Cappello, S., Denaro, R., and Golyshin, P.N. (2007a) Microbial Community of a Hydrothermal Mud Vent Underneath the Deep-Sea Anoxic Brine Lake Urania (Eastern Mediterranean). Orig Life Evol Biosph 37: 177–188.

Yakimov, M.M., La Cono, V., Denaro, R., D'Auria, G., Decembrini, F., Timmis, K.N. et al. (2007b) Primary producing prokaryotic communities of brine, interface and seawater above the halocline of deep anoxic lake L'Atalante, Eastern Mediterranean Sea. ISME J 1: 743–755.

Zengler, K., Richnow, H.H., Rossello-Mora, R., Michaelis, W., and Widdel, F. (1999) Methane formation from long-chain alkanes by anaerobic microorganisms. Nature 401: 266-269.

Zepp Falz, K., Holliger, C., Grosskopf, R., Liesack, W., Nozhevnikova, A.N., Müller, B., Wehrli, B., and Hahn, D. (1999) Vertical Distribution of Methanogens in the Anoxic Sediment of Rotsee (Switzerland). Appl Environ Microbiol 65: 2402–2408.

Zhilina, T.N., and Zavarzin, G.A. (1990) Extremely halophilic, methylotrophic, anaerobic bacteria. FEMS Microbiol Rev 87: 315-322.

Zhou, J., Bruns, M.A., and Tiedje, J.M. (1996) DNA recovery from soils of diverse composition. Appl Environ Microbiol 62: 316-322.

Phylogenetic affiliation	DGGE band	Closest uncultured relative (accession number) and origin	Sequence identity (%)
MBG-D	NapK-dggeB4 (0-20 cmbsf)	SMI1-GC205-Arc25 (DQ521770) Hypersaline Sediments, Gulf of Mexico	100
	NapK-dggeB10 (80-100 cmbsf)	SMI1-GC205-Arc38 (DQ521781) Hypersaline Sediments, Gulf of Mexico	98
ANME-1	NapK-dggeB1 (0-20 cmbsf)	V.8.ArB20 (AY367348) Seawater and Sediments of the Cascadia Margin	98
	NapK-dggeB2 (0-20 cmbsf)	SMI2-GC205-Arc61 (DQ521758) Hypersaline Sediments, Gulf of Mexico	99
	NapK-dggeB3 (0-20 cmbsf)	A163B12 (FJ455954) SMTZ, Santa Barbara Basin, California	97
	NapK-dggeB5 (20-40 cmbsf)	BA1b1 (AF134382) Eel River Basin, Northern California	98
	NapK-dggeB6 (20-40 cmbsf)	V.8.ArB20 (AY367348) Seawater and Sediments of the Cascadia Margin	96
ANME-2	NapK-dggeB7 (60-80 cmbsf)	Kazan-3A-05 (AY592029) Kazan Mud Volcano, Mediterrenean Sea	98
	NapK-dggeB8 (60-80 cmbsf)	a149 (FM179915) Gullfaks and Tommeliten Methane Seeps, Northern North Sea	98
ANME-3	NapK-dggeB9 (60-80 cmbsf)	R45_1d_E12 (EU084525) Sediments from a deep-sea whale-fall in Monterey Canyon	98

Table 1. Closest 16S rRNA gene sequences matches to the dominant DGGE excised bands detected by nested PCR-DGGE in the Napoli center sediments, using the NCBI BLASTN search.

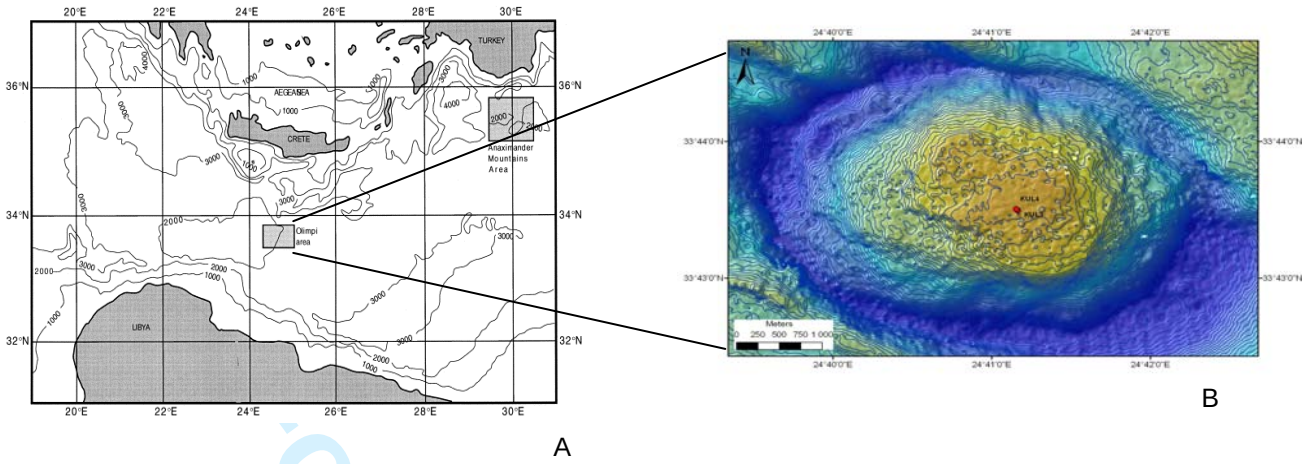

Figure 1. A) Location map showing the Olimpi area in the Eastern Mediterranean Sea. From Aloisi et al. (2000). B) Closer view of the Napoli mud volcano and the sampled gravity cores KUL-3, and KUL-4 (Bénédicte Ritt, pers. comm.).

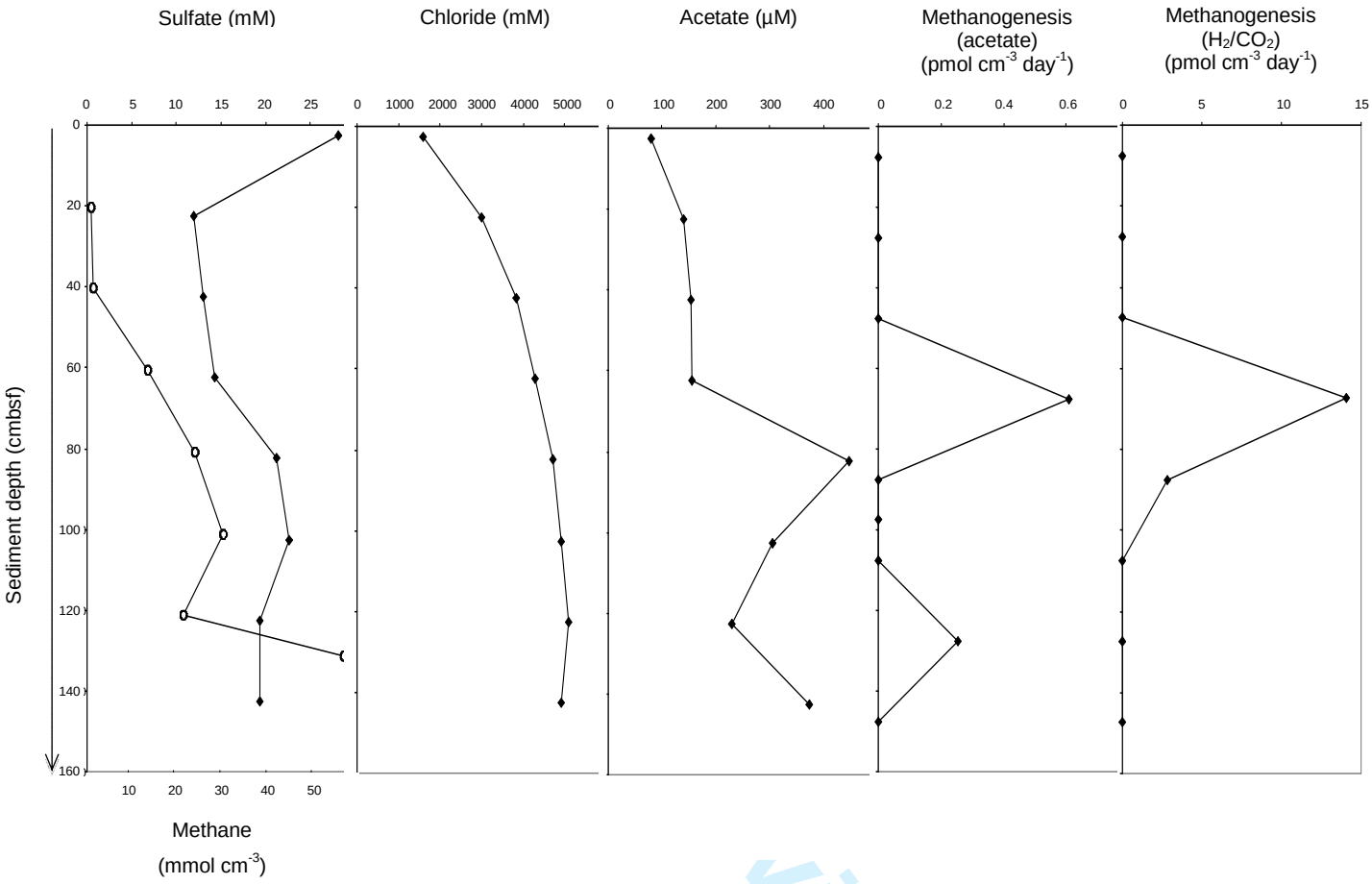

Figure 2. Depth profiles of geochemistry and methanogenic activities in the Napoli mud volcano center sediments. Filled diamonds are sulfate concentrations, and open circles are methane concentrations in mmol per cm^3 of sediment. The scale represents sediment depth below the seafloor.

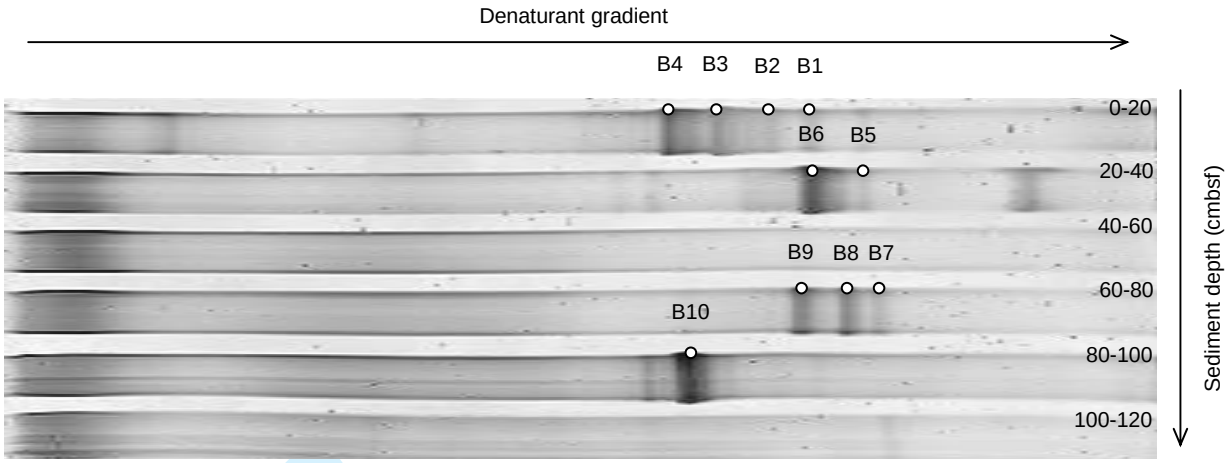

Figure 3. DGGE analysis of archaeal 16S rRNA gene sequences from various sediment depths of the Napoli mud volcano. Numbers B1 to B10 (white dots) are bands corresponding to NapK-dggeB1 to NapK-dggeB10, excised from the gel.

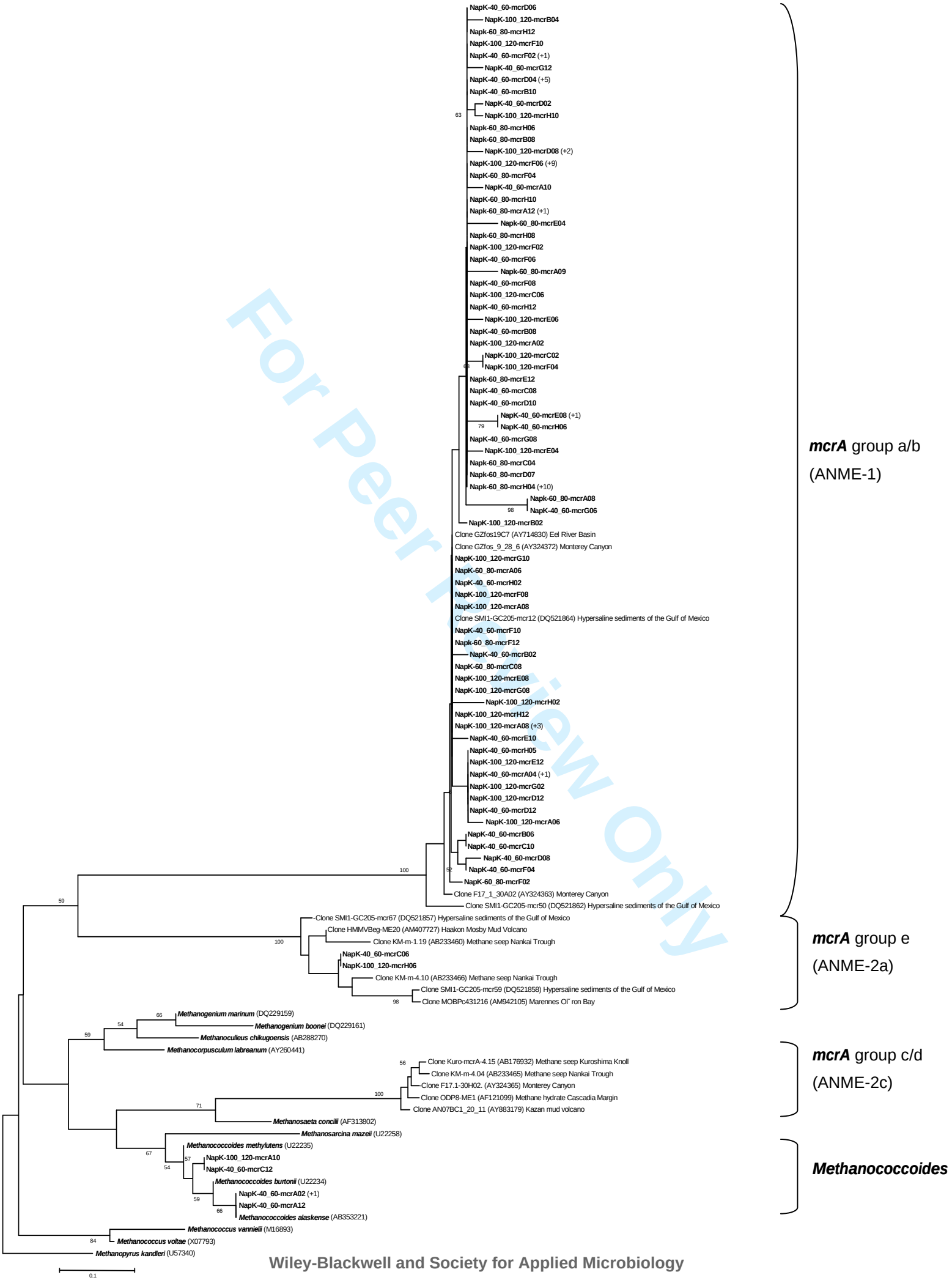

Figure 4. Phylogenetic analysis of MCR amino acid sequences from the center of the Napoli mud volcano sediments based on the neighbour-joining method with approximately 258 amino acid positions. Boostrap values (in percent) are based on 1000 replicates and are indicated at nodes for branches values ≥50% boostrap support. Gene sequences from the Napoli mud volcano sediments are in boldface. Clones with designation beginning NapK-40_60 are from section 40 to 60 cmbsf, clones with designation NapK-60_80 are from section 60 to 80 cmbsf, and clones with designation NapK-100_120 are from section 100 to 120 cmbsf. Numbers in brackets indicate the number of analyzed clones that have more than 97% sequence identity.

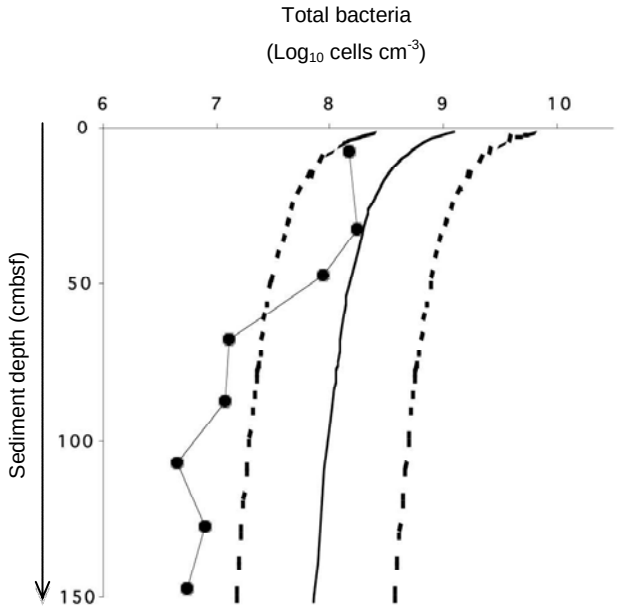

Figure 5. Depth profile of total prokaryotic cells in the Napoli mud volcano center sediments. The black line represents a general regression equation based on total prokaryotic cell counts from diverse marine sediments, with upper and lower prediction limits (95 %) shown by dashed lines, from Parkes et al**.** (2000).

SUPPLEMENTARY MATERIAL

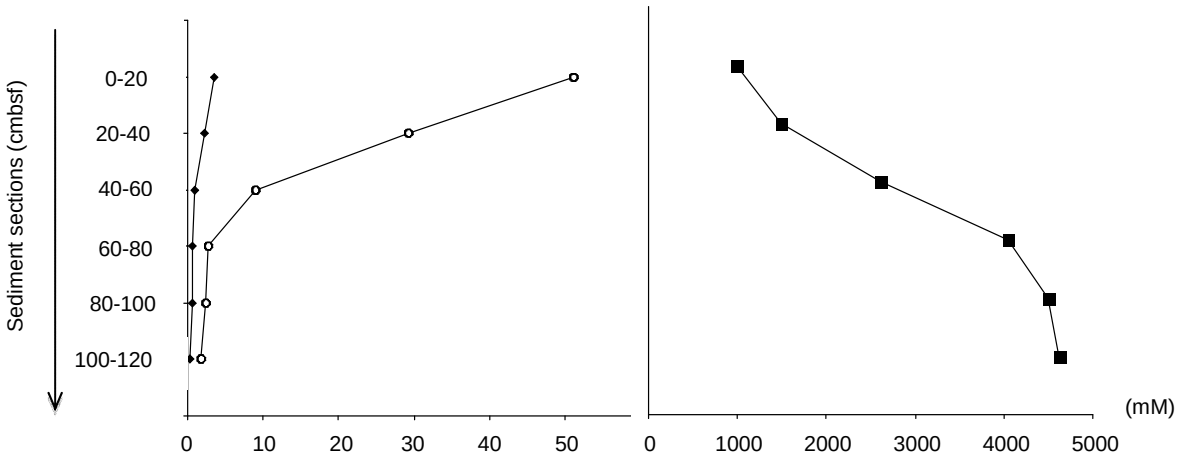

SM1. Depth profiles of the porewater concentrations of Mg^{2+} (open circles), Na^{+} (filled squares), and Ca^{2+} (filled diamonds) in the Napoli mud volcano centre sediment sections.

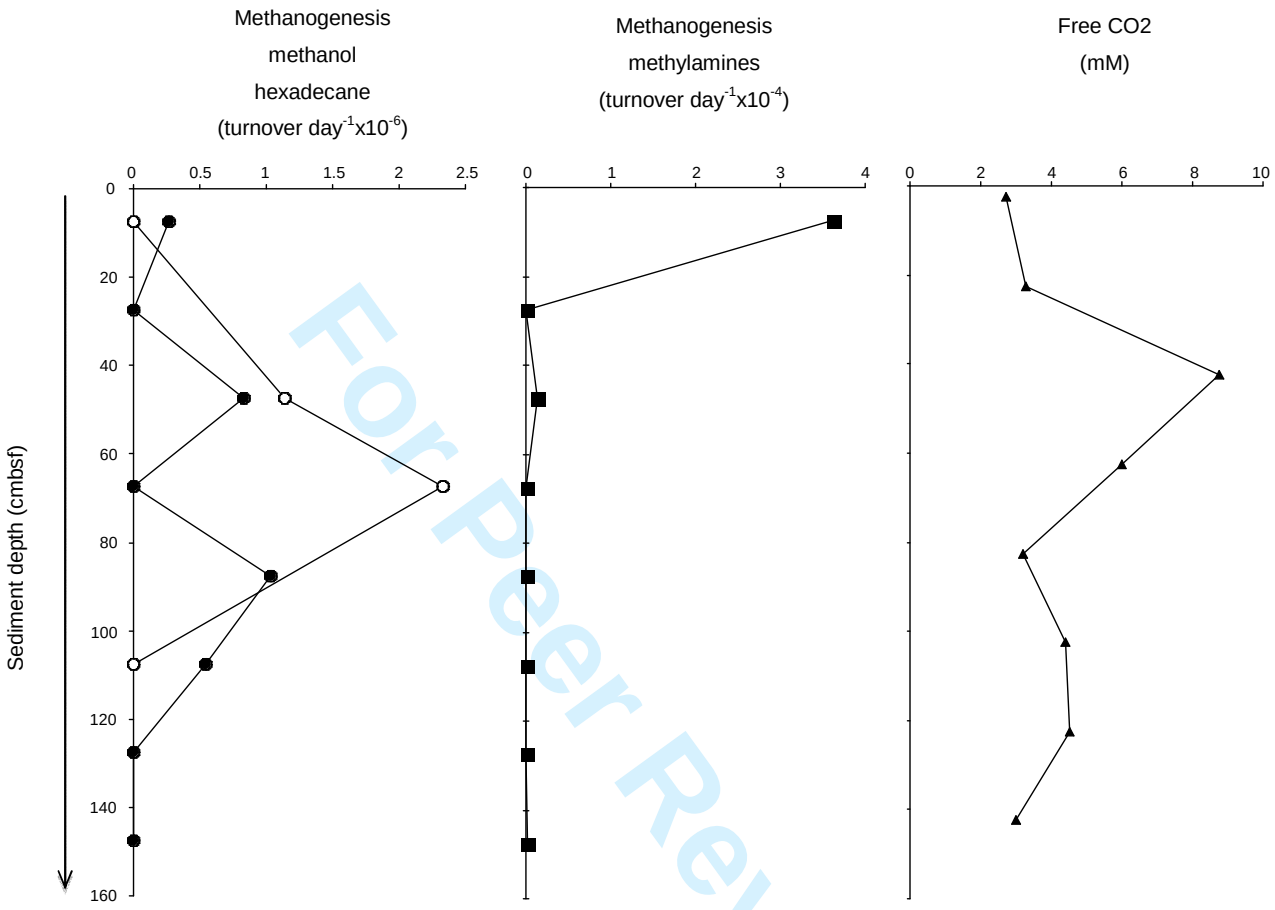

SM2. Depth profiles of methanogenic activities from methylamines, methanol (filled circles) and hexadecane (open circles), and free CO_2 in the Napoli mud volcano center sediments. Methanogenic rates are expressed in turnover/day.

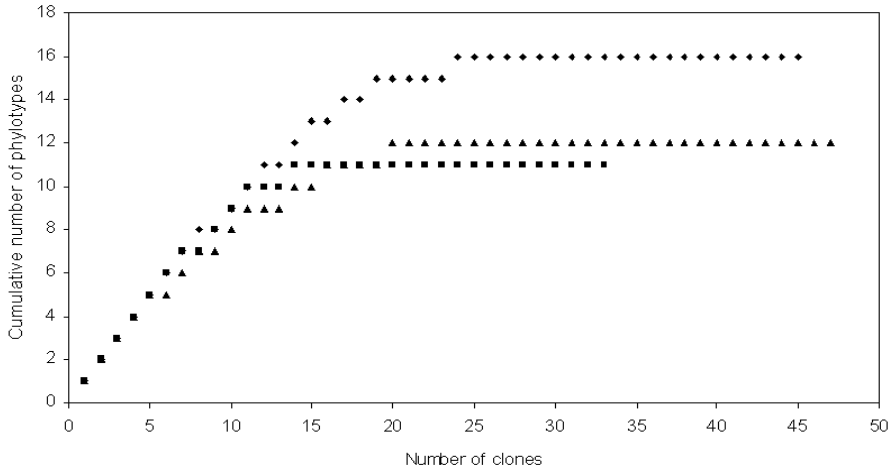

SM3. Rarefaction analysis of the ***mcrA*** gene libraries sections 40-60 cmbsf (filled triangles), 60-80 cmbsf (filled squares), and 100-120 cmbsf (filled diamonds), done using the RarFac program.

Phylogenetic affiliation	Clone	Closest uncultured relative (accession number) and origin	Sequence identity (%)
Methanococcoides	NapK-40_60-mcrA02	strain DSM 17273 (AB353221) ***Methanococcoides alaskense***	99
	NapK-40_60-mcrA12	strain DSM 17273 (AB353221) ***Methanococcoides alaskense***	99
	NapK-100_120-mcrA10	MOBOcr43040 (AM942090) Gassy Subsurface Sediments of Marennes-Oleron Bay	86
mcrA group e	NapK-40_60-mcrC06	SMI1-GC205-mcr67 (DQ521857) Hypersaline Sediments, Gulf of Mexico	94
	NapK-100_120-mcrH06	KM-m-4.10 (AB233466) Sediments from methane seeps of the Nankai Trough	97
mcrA group a/b	NapK-40_60-mcrA04	SMI1-GC205-mcr12 (DQ521864) Hypersaline Sediments, Gulf of Mexico	97
	NapK-40_60-mcrA10	F17.1_30A02 (AY324363) Microcosm Enrichment, Monterey Canyon	93
	NapK-40_60-mcrB02	F17.1_30A02 (AY324363) Microcosm Enrichment, Monterey Canyon	93
	NapK-40_60-mcrB06	F17.1_30A02 (AY324363) Microcosm Enrichment, Monterey Canyon	92
	NapK-40_60-mcrB08	F17.1_30A02 (AY324363) Microcosm Enrichment, Monterey Canyon	92
	NapK-40_60-mcrB10	F17.1_30A02 (AY324363) Microcosm Enrichment, Monterey Canyon	93
	NapK-40_60-mcrC08	F17.1_30A02 (AY324363) Microcosm Enrichment, Monterey Canyon	92
	NapK-40_60-mcrC10	F17.1_30A02 (AY324363) Microcosm Enrichment, Monterey Canyon	92
	NapK-40_60-mcrD02	F17.1_30A02 (AY324363) Microcosm Enrichment, Monterey Canyon	92
	NapK-40_60-mcrD04	F17.1_30A02 (AY324363) Microcosm Enrichment, Monterey Canyon	93
	NapK-40_60-mcrD06	F17.1_30A02 (AY324363) Microcosm Enrichment, Monterey Canyon	92
	NapK-40_60-mcrD08	F17.1_30A02 (AY324363) Microcosm Enrichment, Monterey Canyon	93
	NapK-40_60-mcrD10	F17.1_30A02 (AY324363) Microcosm Enrichment, Monterey Canyon	92
	NapK-40_60-mcrD12	SMI1-GC205-mcr12 (DQ521864) Hypersaline Sediments, Gulf of Mexico	96
	NapK-40_60-mcrE08	F17.1_30A02 (AY324363) Microcosm Enrichment, Monterey Canyon	92
	NapK-40_60-mcrE10	F17.1_30A02 (AY324363) Microcosm Enrichment, Monterey Canyon	95
	NapK-40_60-mcrF02	F17.1_30A02 (AY324363) Microcosm Enrichment, Monterey Canyon	93
	NapK-40_60-mcrF04	F17.1_30A02 (AY324363) Microcosm Enrichment, Monterey Canyon	93
	NapK-40_60-mcrF06	F17.1_30A02 (AY324363) Microcosm Enrichment, Monterey Canyon	92
	NapK-40_60-mcrF08	F17.1_30A02 (AY324363) Microcosm Enrichment, Monterey Canyon	92
	NapK-40_60-mcrF10	F17.1_30A02 (AY324363) Microcosm Enrichment, Monterey Canyon	95
	NapK-40_60-mcrG06	F17.1_30A02 (AY324363) Microcosm Enrichment, Monterey Canyon	87
	NapK-40_60-mcrG08	F17.1_30A02 (AY324363) Microcosm Enrichment, Monterey Canyon	93
	NapK-40_60-mcrG12	F17.1_30A02 (AY324363) Microcosm Enrichment, Monterey Canyon	92
	NapK-40_60-mcrH02	F17.1_30A02 (AY324363) Microcosm Enrichment, Monterey Canyon	93
	NapK-40_60-mcrH05	SMI1-GC205-mcr12 (DQ521864) Hypersaline Sediments, Gulf of Mexico	96
	NapK-40_60-mcrH08	F17.1_30A02 (AY324363) Microcosm Enrichment, Monterey Canyon	95
	NapK-40_60-mcrH12	F17.1_30A02 (AY324363) Microcosm Enrichment, Monterey Canyon	93
	NapK-60_80-mcrA06	GZfos_9_28.6 (AY324372) Microcosm Enrichment, Monterey Canyon	98
	NapK-60_80-mcrA08	F17.1_30A02 (AY324363) Microcosm Enrichment, Monterey Canyon	87
	NapK-60_80-mcrA09	F17.1_30A02 (AY324363) Microcosm Enrichment, Monterey Canyon	91
	NapK-60_80-mcrA12	F17.1_30A02 (AY324363) Microcosm Enrichment, Monterey Canyon	93
	NapK-60_80-mcrB08	F17.1_30A02 (AY324363) Microcosm Enrichment, Monterey Canyon	92

NapK-60_80-mcrC04	F17.1_30A02 (AY324363)	92
NapK-60_80-mcrC08	Microcosm Enrichment, Monterey Canyon F17.1_30A02 (AY324363)	95
NapK-60_80-mcrD07	Microcosm Enrichment, Monterey Canyon F17.1_30A02 (AY324363)	92
NapK-60_80-mcrE04	Microcosm Enrichment, Monterey Canyon F17.1_30A02 (AY324363)	92
NapK-60_80-mcrE12	Microcosm Enrichment, Monterey Canyon F17.1_30A02 (AY324363)	92
NapK-60_80-mcrF02	Microcosm Enrichment, Monterey Canyon F17.1_30A02 (AY324363)	96
NapK-60_80-mcrF04	Microcosm Enrichment, Monterey Canyon F17.1_30A02 (AY324363)	93
NapK-60_80-mcrF12	Microcosm Enrichment, Monterey Canyon F17.1_30A02 (AY324363)	93
NapK-60_80-mcrH04	Microcosm Enrichment, Monterey Canyon F17.1_30A02 (AY324363)	93
NapK-60_80-mcrH06	Microcosm Enrichment, Monterey Canyon F17.1_30A02 (AY324363)	92
NapK-60_80-mcrH08	Microcosm Enrichment, Monterey Canyon F17.1_30A02 (AY324363)	92
NapK-60_80-mcrH10	Microcosm Enrichment, Monterey Canyon F17.1_30A02 (AY324363)	93
NapK-60_80-mcrH12	Microcosm Enrichment, Monterey Canyon F17.1_30A02 (AY324363)	92
NapK-100_120-mcrA02	Microcosm Enrichment, Monterey Canyon F17.1_30A02 (AY324363)	92
NapK-100_120-mcrA06	Microcosm Enrichment, Monterey Canyon SMI1-GC205-mcr12 (DQ521864)	95
NapK-100_120-mcrA08	Hypersaline Sediments, Gulf of Mexico GZfos_9_28.6 (AY324372)	97
NapK-100_120-mcrB02	Microcosm Enrichment, Monterey Canyon GZfos_9_28.6 (AY324372)	97
NapK-100_120-mcrB04	Microcosm Enrichment, Monterey Canyon F17.1_30A02 (AY324363)	92
NapK-100_120-mcrC02	Microcosm Enrichment, Monterey Canyon F17.1_30A02 (AY324363)	92
NapK-100_120-mcrC06	Microcosm Enrichment, Monterey Canyon F17.1_30A02 (AY324363)	93
NapK-100_120-mcrD08	Microcosm Enrichment, Monterey Canyon F17.1_30A02 (AY324363)	93
NapK-100_120-mcrD12	Microcosm Enrichment, Monterey Canyon SMI1-GC205-mcr12 (DQ521864)	96
NapK-100_120-mcrE04	Hypersaline Sediments, Gulf of Mexico F17.1_30A02 (AY324363)	92
NapK-100_120-mcrE06	Microcosm Enrichment, Monterey Canyon F17.1_30A02 (AY324363)	92
NapK-100_120-mcrE08	Microcosm Enrichment, Monterey Canyon F17.1_30A02 (AY324363)	95
NapK-100_120-mcrE12	Microcosm Enrichment, Monterey Canyon SMI1-GC205-mcr12 (DQ521864)	94
NapK-100_120-mcrF02	Hypersaline Sediments, Gulf of Mexico F17.1_30A02 (AY324363)	92
NapK-100_120-mcrF04	Microcosm Enrichment, Monterey Canyon F17.1_30A02 (AY324363)	92
NapK-100_120-mcrF06	Microcosm Enrichment, Monterey Canyon F17.1_30A02 (AY324363)	93
NapK-100_120-mcrF08	Microcosm Enrichment, Monterey Canyon F17.1_30A02 (AY324363)	96
NapK-100_120-mcrF10	Microcosm Enrichment, Monterey Canyon F17.1_30A02 (AY324363)	92
NapK-100_120-mcrG02	Microcosm Enrichment, Monterey Canyon F17.1_30A02 (AY324363)	96
NapK-100_120-mcrG06	Microcosm Enrichment, Monterey Canyon F17.1_30A02 (AY324363)	92
NapK-100_120-mcrG08	Microcosm Enrichment, Monterey Canyon GZfos_9_28.6 (AY324372)	98
NapK-100_120-mcrG10	Microcosm Enrichment, Monterey Canyon GZfos_9_28.6 (AY324372)	97
NapK-100_120-mcrH02	Microcosm Enrichment, Monterey Canyon F17.1_30A02 (AY324363)	93
NapK-100_120-mcrH10	Microcosm Enrichment, Monterey Canyon F17.1_30A02 (AY324363)	92
NapK-100_120-mcrH12	Microcosm Enrichment, Monterey Canyon F17.1_30A02 (AY324363)	94
	Microcosm Enrichment, Monterey Canyon	

SM4. Closest relatives of representative clones from ***mcrA*** gene libraries from depths 40 to 60 cmbsf (NapK-40_60), 60 to 80 cmbsf (NapK-60_80), 100 to 120 cmbsf (Napk-100_120) for the Napoli mud volcano.